Journal of Magnetism and Magnetic Materials 570 (2023) 170371

Contents lists available at ScienceDirect

Journal of Magnetism and Magnetic Materials

journal homepage: www.elsevier.com/locate/jmmm

Revealing anti-ferromagnetic domains with linear non-reciprocal optical effects

X.D. Zhu *

Department of Physics and Astronomy, University of California, Davis, CA 95616, USA
Department of Optical Sciences and Engineering, Fudan University, Shanghai 200045, China

ARTICLE INFO

Keywords:
Antiferromagnetic materials
Magnetic domains
Magneto-optics
Sagnac interferometry
Scanning microscopy
Non-reciprocal linear optical effects

ABSTRACT

I show that domains in anti-ferromagnetic crystals that break inversion symmetry as well as time-reversal symmetry can be characterized using linear non-reciprocal optical effects detected with Sagnac-interferometry-based microscopy. In addition, a simultaneous detection of these effects from oppositely aligned domains yields a background-free measurement of non-reciprocal optical susceptibilities.

There exists a class of antiferromagnetic (AFM) materials in which both time-reversal symmetry and global inversion symmetry are broken [1 –4]. In these materials, linear and non-linear non-reciprocal (NR) optical effects (i.e., effects that change under the time-reversal operation) arise. The corresponding NR optical susceptibilities serve as convenient order parameters for such AFM materials, just as usual magnetic susceptibilities for ferromagnetic (FM) materials. Here linearity and non-linearity of the effects refer to the dependence on the illuminating electric field at optical frequencies, not the magnetization in a sample. Non-reciprocal (NR) optical effects here refer to an optically induced magnetization by an illuminating electric field at an optical frequency and an optically induced electric polarization by an illuminating magnetic field at an optical frequency, afforded by the broken symmetries. These effects produce measurable magneto-optic effects. Thus even in the absence of a net magnetization, NR optical susceptibilities are effective parameters to characterize AFM phase transition and domains with or without externally applied dc or low frequency fields.

Cr_2O_3 is the first AFM material of this class in which both linear and second-order nonlinear NR optical effects have been investigated. Pisarev *et al.* were the first to measure linear NR optical effects in *transmission* in a Cr_2O_3 single crystal at wavelength of 1.15 μm by detecting the Faraday rotation through the sample in the absence of external dc electric field and magnetic field [5]. In their study, the sample is polarized into a single AFM domain by simultaneous application of a dc electric field and a dc magnetic field. The polarizing fields are then removed before the Faraday rotation through the sample is detected. Such a linear NR optical effect is distinguished from a linear magneto-electric (ME) effect induced by a dc or low-frequency electric-field [5 –7]. A linear ME effect refers to induction of a magnetization by a dc or low-frequency electric field in a material that breaks both time-reversal symmetry and inversion symmetry, such as an anti-ferromagnetic Cr_2O_3 single crystal. Such a magnetization can be polarized or oriented with a dc magnetic field. It produces a magneto-optic effect, just like a spontaneous magnetization in a ferromagnetic material. Krichevtsov *et al.* were the first to measure the linear NR optical effect in *reflection* from Cr_2O_3 single crystal samples at wavelength of 0.633 μm [6]. Again these authors polarized the sample into a single AFM domain by cooling it to below the Neel temperature in simultaneously applied dc electric field and dc magnetic field. During subsequent optical reflection measurements, the applied fields were removed. The linear NR optical effect in Cr_2O_3 at 0.633 μm is enhanced by the spin-allowed $^4A_2 \rightarrow {}^4T_2$ electronic transition [8,9]. So far linear NR optical effects have not been used to image domains in AFM materials after these earlier work. It is known that such NR optical effects associated with an AFM order state are weak and often accompanied by much larger reciprocal optical effects (i.e., effects that remain unchanged under the time reversal operation), thus making AFM domain imaging using linear NR optical effects most difficult if backgrounds are not suppressed [10].

Fiebig *et al.* were the first to report measurements of second-order nonlinear NR optical effects by taking advantage of a combination of

* Address: Department of Physics and Astronomy, University of California, Davis, CA 95616, USA.
E-mail address: xdzhu@physics.ucdavis.edu.

https://doi.org/10.1016/j.jmmm.2023.170371
Received 17 October 2022; Received in revised form 24 December 2022; Accepted 5 January 2023
Available online 7 January 2023

broken inversion symmetry, electronic resonance enhancement involving spin-allowed $^4A_2 \rightarrow {}^4T_2$ and $^4T_1$ transitions, and the interference between the nonlinear NR optical effect and a reciprocal optical effect [11]. Unlike linear NR optical effect measurements that are plagued by large reciprocal optical effects, the latter are suppressed at optical second-harmonics by symmetry. As a result, these authors were able to image AFM domains in Cr_2O_3 single crystals using the second-order nonlinear NR optical effects.

In this work, I report an experimental study of linear NR optical effects in Cr_2O_3 using a zero-area Sagnac-interferometry-based microscope at wavelength 0.79 μm [12]. A zero-area Sagnac interferometry measures the difference between phases accumulated by two optical beams that traverse through a loop but in opposite directions. Since the phase acquired due to reciprocal optical effects is identical while the phase accumulated due to NR optical effects is same but having opposite signs, the interferometry suppresses reciprocal optical effects to extinction while detecting linear NR optical effects doubly well [13]. In the current microscope, a linear NR optical effect is detected with a sensitivity below 10^{-7} radians. I report the first linear NR effect image of AFM domains in a Cr_2O_3 crystal measured without electronic resonance enhancement. Furthermore I demonstrate that simultaneous detection of these linear optical effects from AFM domains of opposite alignments yields a nearly background-free measurement of linear NR optical susceptibilities that signify the paramagnetic-antiferromagnetic phase transition. This work is significant for its being generally applicable to investigating other AFM materials with broken inversion symmetry in their antiferromagnetic states.

Specific to a Cr_2O_3 single crystal, above the Neel temperature at $T_N = 307$ K, it is a centrosymmetric material belonging to point group D_{3d}. Below T_N, spins in the unit cell are ordered along the c-axis (the optic axis) to assume a noncentrosymmetric structure belonging to point group D_3 [9,14]. As a result, linear NR optical effects emerge in the AFM state. These effects are gyrotropic and result from an electric polarization induced by the magnetic dipole interaction [6], $\boldsymbol{P}_i = (\epsilon_0 c)\alpha^{(ME)}_{ij,MD}$: $\boldsymbol{B}_j$, and an emergent magnetic polarization induced by the electric dipole interaction, $\boldsymbol{M}_i = (\epsilon_0 c)\alpha^{(ME)}_{ij,ED}$: $\boldsymbol{E}_j$. If the c-axis is chosen as the z-axis, $\alpha^{(ME)}_{ij,MD}$ and $\alpha^{(ME)}_{ij,ED}$ only have diagonal elements. When effects on transmission and reflection are considered, these linear NR optical susceptibilities add anti-symmetric off-diagonal terms to the optical dielectric tensor [5]. In this work, I study optical reflection at normal incidence from a $Cr_2O_3(0001)$ sample with the c-axis along the surface normal. In this case, the unit vector of propagation for the illuminating optical beam, $\hat{k} = (0,0,1)$ points into the sample. The corresponding correction to the dielectric tensor is given by [15]

$$\overleftrightarrow{\delta\varepsilon} = \sqrt{\varepsilon}\begin{pmatrix} 0 & -\alpha^{(ME)}_{xx,MD} + \alpha^{(ME)}_{xx,ED} & 0 \\ \alpha^{(ME)}_{xx,MD} - \alpha^{(ME)}_{xx,ED} & 0 & 0 \\ 0 & 0 & 0 \end{pmatrix} \quad (1)$$

To use the same notation for the net linear NR optical susceptibility as adopted by Krichevtsov *et al.* [6], I define $\alpha_{xx} \equiv (\alpha^{(ME)}_{xx,MD} - \alpha^{(ME)}_{xx,ED})\sqrt{\epsilon}/2$. Following a general approach described by the author in an earlier work [15], the linear NR optical effects add off-diagonal terms to the normal-incidence reflection matrix as follows [16]:

$$\mathbb{R} = \begin{pmatrix} -\left(\sqrt{\epsilon}-1\right)\Big/\left(\sqrt{\epsilon}+1\right) & 2\alpha_{xx}\Big/\left(\sqrt{\epsilon}+1\right)^2 \\ -2\alpha_{xx}\Big/\left(\sqrt{\epsilon}+1\right)^2 & -\left(\sqrt{\epsilon}-1\right)\Big/\left(\sqrt{\epsilon}+1\right) \end{pmatrix} \quad (2)$$

or

$$\mathbb{R} = \begin{pmatrix} r_n & \Delta \\ -\Delta & r_n \end{pmatrix} \quad (3)$$

$\Delta \equiv 2\ \alpha_{xx}/(\sqrt{\epsilon}+1)^2$. $r_n \equiv -(\sqrt{\epsilon}-1)/(\sqrt{\epsilon}+1)$ is the Fresnel reflection coefficient at normal incidence. I note here that in the AFM state there exists a magnetic linear birefringence effect in a $Cr_2O_3(0001)$ sample [5]. Such an effect adds small diagonal elements to the dielectric tensor in Equation (1). At normal incidence, they change r_n in the range of 10^{-3} [15]. As a result, they have a negligible effect on the measurement of off-diagonal elements $\alpha^{(ME)}_{xx,MD} - \alpha^{(ME)}_{xx,ED}$ [17]. I further note here that residual symmetric off-diagonal matrix elements in the dielectric tensor [5] and the Voigt effect [18] yield symmetric off-diagonal terms in the normal-incidence reflection matrix [15]. A normal-incidence Sagnac interferometer measures the difference between off-diagonal terms in the reflection matrix [17]. As a result, these symmetric off-diagonal terms in the dielectric tensor do not contribute to signals detected with such a Sagnac interferometry employed in the present study.

On a $Cr_2O_3(0001)$ sample, 180° domains are distinguishable from one another by a time-reversal symmetry operation. Such an operation changes the sign of α_{xx} and an image of a $Cr_2O_3(0001)$ sample in α_{xx} or Δ/r_n reveals 180° domains as bright and dark regions. In the present investigation, two $Cr_2O_3(0001)$ plates from Surface Preparation Laboratory (Zaandam, the Netherlands) are used: one is of 3 $mm \times 3$ $mm \times 1$ mm, and the other of 3 $mm \times 3$ $mm \times 0.5$ mm. These sample plates are mechanically polished to an optical finish by the vendor and are not further treated.

To measure these linear NR optical effects, I use a zero-area Sagnac-interferometry-based scanning microscope [12]. As shown in Fig. 1, by focusing the illumination beam on the front surface of a sample, the microscope is operated in Kerr mode so that only the reflection from the front surface is analyzed. In this case, the microscope measures the real part of Δ/r_n, namely, $Re\{-2\alpha_{xx}/(\epsilon-1)\}$ [15]. The spatial resolution is variable from 0.85 μm to 13 μm by using different objectives. The sensitivity of the present microscope is $2 \times 10^{-7}/\sqrt{Hz}$ radians, sufficient for detecting linear NR optical effects in Cr_2O_3 crystals.

In Fig. 2, I show an image of a 2.44 $mm \times 2.44$ mm area on the 3 $mm \times 3$ $mm \times 1$ mm $Cr_2O_3(0001)$ sample in $Re\{\Delta/r_n\}$ acquired at T = 293 K, after the as-received sample is annealed to 310 K over the Neel temperature briefly. The scan step size in both the vertical and horizontal directions is 13 μm and the dwelling time constant at each pixel is 100 ms. At T = 310 K, the image (not shown here) has no feature and is at the noise level of the detection, i.e., 4×10^{-7} radians. The image in Fig. 2 reveals two 180° AFM domains. The absolute signals in these two domains are comparable, $\cong 4 \times 10^{-6}$ radians. In the insert, I show a high-resolution, low-noise image over a $17\mu m \times 17$ μm region near the center of the large image. It is acquired with a spatial resolution of 0.85 μm and a time constant of 3 s. It shows that the domain wall is step-like limited by the spatial resolution. Within each domain, $Re\{\Delta/r_n\}$ is uniform with a noise floor of 1.1×10^{-7} radians. There is a slow drift in signal in the large image. It is originated from residual non-reciprocal as well as reciprocal optical effects in the microscope system [10]. They are insignificant compared to the main features in the image.

To measure the linear NR optical susceptibilities α_{xx} from single domains as functions of temperature, I measured $Re\{\Delta/r_n\}$ from two points on the sample (see marks in Fig. 2) from 308 K to 80 K: one point in the dark region with $\alpha_{xx} > 0$ and the other in the bright region with $\alpha_{xx} < 0$. The results are shown in Fig. 3. The curves from two 180° domains are more or less symmetric about zero, as expected. In the measured values of $Re\{\Delta/r_n\}$, there are contributions from residual reciprocal and NR optical effects that are not associated with the sample. These backgrounds drift during the measurement. To remove them, I take the difference of the two curves in Fig. 3. This removes the common backgrounds to a level below the amplifier noise while keeping only the effect due to α_{xx}. Dividing the difference by 2 yields $Re\{-2\alpha_{xx}/(\epsilon-1)\}$ and the result is shown in Fig. 4. It is a background-free measurement of the linear NR optical effect over a wide range of temperature and describes the paramagnetic-antiferromagnetic phase transition in $Cr_2O_3(0001)$.

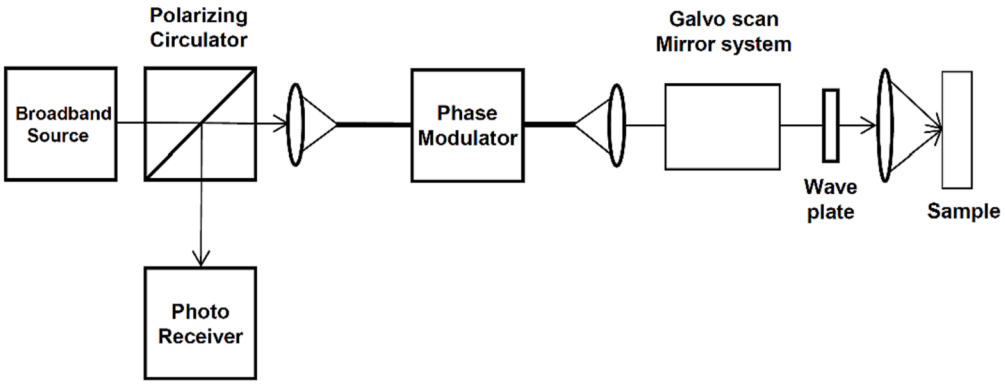

Fig. 1. Sketch of the normal-incidence zero-area Sagnac interferometric scanning microscope used in this work. A galvo scan mirror system changes the yaw and the pitch of the beam before an objective to achieve the scan across the sample along the horizontal direction (x-axis) and the vertical direction (y-axis).

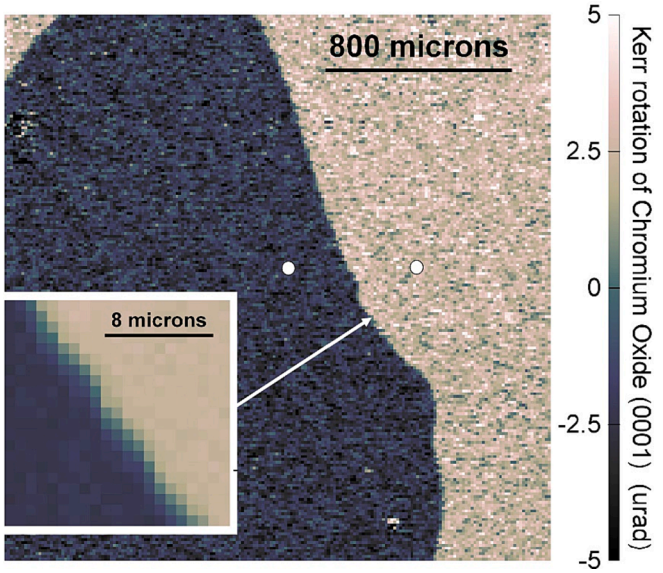

Fig. 2. Polar Kerr image of 1 mm × 3 mm × 3 mm Cr_2O_3(0001) after annealing to 320 K with a resolution of 12.75 μm. It is different from the image when the sample was first received, indicating that domain walls have moved. The inlet is a zoom-in image near the center of the large image with a resolution of 0.85 μm. The two white dots mark the locations where Kerr rotation signals as functions of temperature are simultaneously measured.

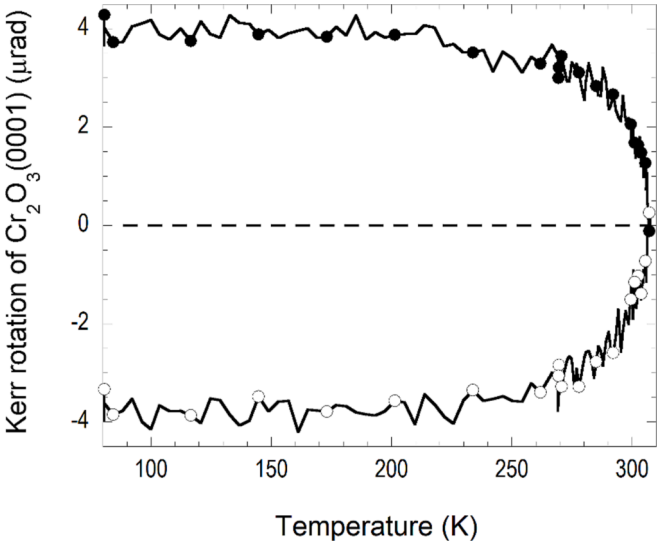

Fig. 3. $Re\{\Delta/r_n\}$ from 80 K and 308 K measured from two locations marked in Fig. 2, namely, from two oppositely aligned AFM domains. The line decorated with solid white circles is from the location marked in the dark region, while the line decorated with solid black circles is from the location marked in the bright region.

To further validate that such a procedure is robust, I acquired 4 difference curves in separate measurements done in different days: two during cooling down, two during warming up. As shown in Fig. 5, they reproduce each other within the amplifier noise of $2 \times 10^{-7}/\sqrt{Hz}$ radians in the current microscope. Taking $\sqrt{\epsilon} = 2.5$ as in the work of Krichevtsov et al. [6]. I find $Re\{\alpha_{xx}\} = 1.05 \times 10^{-5}$ at 0.78 μm at T = 80 K. It is a factor of 18 smaller than $Re\{\alpha_{xx}\} = 1.8 \times 10^{-4}$ at 0.633 μm as reported by Krichevtsov *et al.* From a study of optical absorption in Cr_2O_3 crystals reported by McClure [8], the linear NR optical susceptibility at 0.633 μm is electronic resonance-enhanced. Such an enhancement diminishes at 0.78 μm.

I now discuss the results. It is noteworthy that antiferromagnetic domains in Cr_2O_3 crystals (see Fig. 2) are large, in the order of millimeters or larger. This observation agrees with the report of Fiebig *et al.* [11]. Since there is no magnetic energy or stray field energy that needs to be curtailed by having multiple domains, it is not surprising that domains in an AFM crystal are large. The domain wall shown in Fig. 2 has already moved from its position when the sample is first received. The movement is due to annealing to 310 K before the image shown in Fig. 2 is acquired. The second Cr_2O_3(0001) sample initially has three AFM domains when it is first received. After it is annealed to 320 K, the entire sample becomes a single domain below the Neel temperature without having it polarized with any dc external fields. It is noteworthy that imaging AFM domains using second-order nonlinear NR optical effects is subject to variations in surface morphology and beam intensity [11]. Detection of linear NR optical effects with a Sagnac interferometry is much less affected by these variations as $Re\{\Delta/r_n\}$ is extracted through a normalization procedure that removes these variations [13,17]. Fig. 4 demonstrates that α_{xx} can be extracted background-free when $Re\{\Delta/r_n\}$ from two oppositely aligned domains are measured simultaneously. One can then afford to critically examine α_{xx} as an order parameter over a wide range of temperature [14]. In fact, by fitting the curve in Fig. 4 near the transition temperature to a temperature-dependent function of the form $(T_N - T)^{\alpha}$, I find $T_N = 307.2$ K ±0.2K and $\alpha = 0.40$ ±0.02. The value of the exponent is between the value (0.50) expected of the mean-field theory [19] and the value (0.33) predicted by a 3D Ising model [20].

By point group symmetry, a majority of antiferromagnetic crystals have broken inversion symmetry in antiferromagnetic states [21 –23]. For their characterization, emergent linear NR optical effects can be

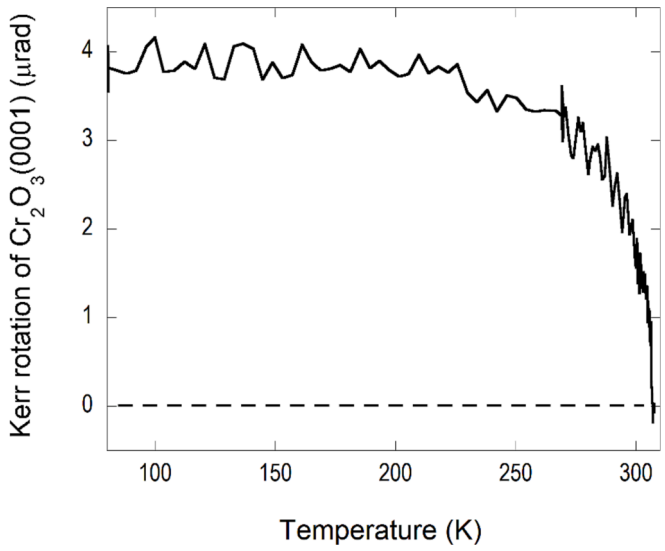

Fig. 4. Difference between two curves in Fig. 3 divided by 2. It is the amplitude of $Re\{-2\alpha_{xx}/(\epsilon-1)\}$ from 80 K to 308 K.

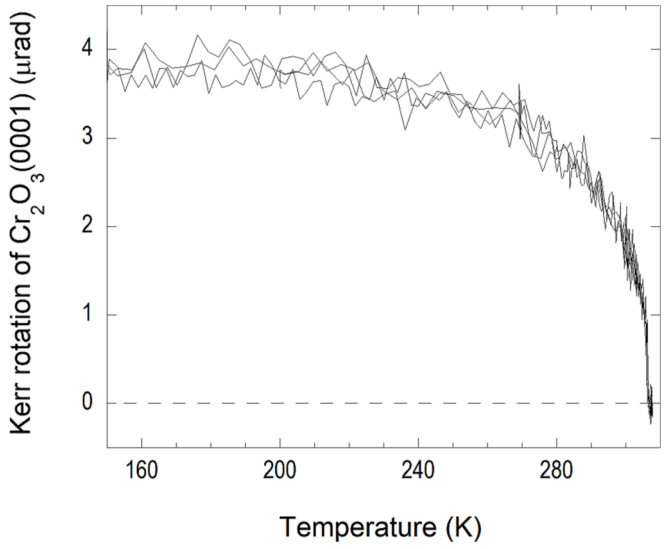

Fig. 5. Difference curves, $Re\{-2\alpha_{xx}/(\epsilon-1)\}$, obtained from 4 separate measurements. They reproduce each other within the amplifier noise.

used as order parameters. Unfortunately, these effects are weak and thus difficult to measure without some form of electronic enhancements and background suppression. The present work shows that these linear NR optical effects can be measured without electronic enhancement by using a zero-area Sagnac interferometry-based microscopy that suppresses linear reciprocal optical effects. The Sagnac microscope in the present study has a sensitivity of $2\times10^{-7}/\sqrt{Hz}$ radians. It is limited by the amplifier noise and a 10-mW super-luminescence light source. If the source is replaced with a source of 30 mW, the sensitivity is immediately improved to $7\times10^{-8}/\sqrt{Hz}$ radians. It means that the image shown in Fig. 2 or a portion of it can be acquired with a sensitivity of 3×10^{-8} radians, and the temperature-dependent $\mathrm{Re}\{\alpha_{xx}\}$ can be measured with a sensitivity of 1×10^{-8} radians. This is sufficient to study linear NR optical effects in most AFM materials that have broken inversion symmetry.

Declaration of Competing Interest

The authors declare that they have no known competing financial interests or personal relationships that could have appeared to influence the work reported in this paper.

Data availability

Data will be made available on request.

References

[1] I. Dzyaloshiski, *J. Exptl. Theoret. Phys.* (U.S.S.R) 37 (881) (1959).
[2] D. Astrov, Soviet Phys. JETP 13 (1961) 729.
[3] R. Hornreich, S. Shtrikman, Phys. Rev. 171 (1968) 1065.
[4] M.S. Dresselhaus, G. Dresselhaus, A. Jorio, Group Theory: Application to the Physics of Condensed Matter, Springer, 2008.
[5] R. Pisarev, B. Krichevtsov, V. Pavlov, Phase Trans.: A Multinational J. 37 (1991) 63.
[6] B. Krichevtsov, V. Pavlov, R. Pisarev, V. Gridnev, J. Phys.: Condes. Matters 5 (1993) 8233.
[7] J. Wang, C. Binek, Phys. Rev. Appli. 5 (2016), 031001.
[8] D. McClure, J. Chem. Phys. 38 (1963) 2289.
[9] M. Fiebig, D. Frohlich, B. Krichevtsov, R. Pisarev, Phys. Rev. Lett. 73 (1994) 2127.
[10] A. Fried, M. Fejer, A. Kapitulnik, Rev. Sci. Instrum. 85 (2014), 103707.
[11] M. Fiebig, D. Frohlich, G. Sluyterman, R. Pisarev, Appl. Phys. Lett. 66 (1995) 2906.
[12] X. Zhu, AIP Adv. 11 (2021), 085214.
[13] J. Xia, P. Beyersdorf, M. Fejer, A. Kapitulnik, Appl. Phys. Lett. 89 (2006), 062508.
[14] V. Muthukumar, R. Valenti, C. Gros, Phys. Rev. B 54 (1996) 433.
[15] X. Zhu, OSA-Continuum 4 (2021) 966.
[16] X. Zhu, H. Zhang, Opt. Lett. 45 (2020) 2439.
[17] X. Zhu, Rev. Sci. Instrum 88 (2017), 083112.
[18] J. McCord, J. Phys. D: Appl. Phys. 48 (2015), 333001.
[19] C. Kittel, Introduction to Solid State Physics, John Wiley & Sons, 1986.
[20] A.J. Liu, M.E. Fisher, Physica A 156 (1989) 35.
[21] J. Godinho, H. Reichlová, D. Kriegner, V. Novák, K. Olejník, Z. Kašpar, Z. Šobáň, P. Wadley, R. Campion, R. Otxoa, P. Roy, J. Železný, T. Jungwirth, J. Wunderlich, *Nat. Commun.* **9** (2018) 4686.
[22] T. Higo, H. Man, D. Gopman, L. Wu, T. Koretsune, O. van 't Erve, Y. Kabanov, D. Rees, Y. Li, M. Suzuki, S. Patankar, M. Ikhlas, C. Chien, R. Arita, R. Shull, J. Orenstein, and S. Nakatsuji, *Nat. Photonics* **12** (2018) 73.
[23] Z. Ni, A. Haglund, H. Wang, B. Xu, C. Bernhard, D. Mandrus, X. Qian, E. Mele, C. Kane, L. Wu, Nat. Nanotechnol. 16 (2021) 782.